Oligonucleotide Analogues with Integrated Bases and Backbones

Part 19

Gelation of Organic Solvents by Self-Complementary A*[s]U(*) Dinucleosides

by **Nicolas Bogliotti**, **Anne Ritter**, **Séverine Hebbe**, and **Andrea Vasella***

Laboratorium für Organische Chemie, ETH Zürich, Wolfgang-Pauli Strasse 10, CH-8093 Zürich
(e-mail: vasella@org.chem.ethz.ch)

The A*[s]U(*) dinucleosides **1** and **2** form thermoreversible gels in organic solvents. The basis of the gelation is the formation of linear aggregates by base pairing following desolvation of the nucleobases. This is evidenced by the absence of gel formation by the *C(6)*-deaminated analogue **3** of **1**, the correlation of gelation with the *anti*-conformation, as preferred for **1**, and the temperature-, concentration-, and time-dependent CD spectra. The gels were also characterized by the minimum gelation concentration, the gel–sol transition (melting) temperature, and rheological properties.

Introduction. – Oligoribonucleotide analogues integrating backbone and bases (ONIBs) possess linking elements between the nucleobases that replace the contiguous backbone of the parent oligonucleotides. ONIBs form linear and/or cyclic duplexes [1], as shown by the association of ethynylene- [2], ethenylene- [3], ethylene- [4], *O*- [5], and *S*-linked [6] self-complementary U*[x]A(*)[1]) and A*[x]U(*) dinucleotide analogues in $CDCl_3$. Formation of cyclic duplexes (*i.e.*, pairing) of self-complementary dinucleotide analogues requires a specific conformation, and depends on the nature of the linking unit, the sequence of the nucleobases, and their substitution at C(6) (uridine) or C(8) (adenosine).

In the course of association studies of *S*-linked dinucleotide analogues one of us discovered that the A*[s]U(*) dimers **1** and **2** [6] form thermoreversible gels in organic solvents revealing a new type of association of these analogues that is observable on a macroscopic scale [7].

Gels are viscoelastic materials usually consisting of a liquid and an immobilizing agent (gelator). No definition takes all their properties into account [8–11], and, according to a famous statement, gels are '*easier to recognize than to define*'. The liquid component can be an organic solvent, as in an organogel [12–14], H_2O, as in a hydrogel

[1]) *Conventions for abbreviated notation:* The substitution at C(6) of pyrimidines and C(8) of purines is denoted by an asterisk (*); for example, A* and U* for hydroxymethylated adenosine and uridine derivatives, resp. U(*) represents both unsubstituted and hydroxymethylated uridine derivative. The replacement of the amino group at C(6) of adenosine by an H-atom is denoted by the letter 'H' in superscript (^{H}); for example, ^{H}A represents *C(6)*-deamino adenosine derivative. The moiety x linking C(8)–CH_2 of unit II and C(5′) of unit I is indicated in square brackets, *i.e.*, [s] for a S-atom.

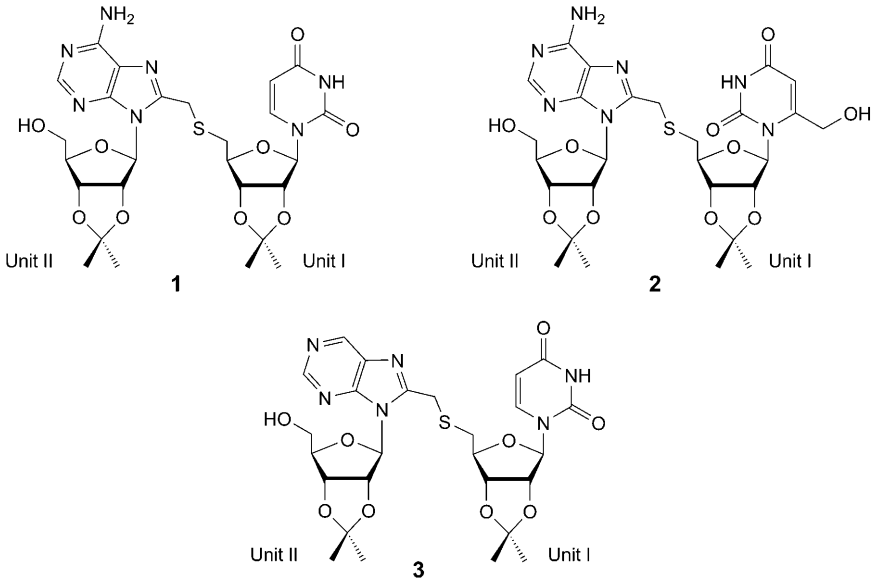

[15–17], or a liquid crystal [18][19]. The gel is characterized by a structure of macroscopic dimensions that is permanent on the time scale of an analytical experiment and by a stress limit below which it shows a solid-like rheological behaviour [20]. The network formed by the gelator prevents the liquid from flowing freely. A gel is either formed irreversibly by covalently cross-linking the gelator, as in a chemical gel, or reversibly to form a physical gel by non-covalent interactions, such as H-bonding, π-π stacking [21], *Van der Waals* forces, and solvophobic effects. Physical gels exhibit a reversible gel–sol transition at a characteristic melting temperature (T_m).

We assumed that the gelation of organic solvents by the dinucleosides **1** and **2** is due to the formation of a network by H-bonding, conceivably leading to base stacking and perhaps assisted by it. To reach a satisfactory level of understanding of the gels, we wished to determine the solvents that are gelled by **1** and **2**, the physico-chemical properties of the gels, the nature of the intermolecular interactions, and the structural elements directly involved in the association. To see whether gelation of solvents by the A*[s]U$^{(*)}$ dimers **1** and **2** requires the formation of H-bonds between the complementary nucleobases rather than between the CH_2OH group(s), we also planned to synthesise the 6-deamino analogue **3** of **1**, and to compare its solubility and ability to gelate solvents to those of **1** and **2**.

Results and Discussion. – 1. *Synthesis of the* ^{H}*A*[s]U Dimer* **3**. We synthesised this dinucleotide analogue from the D-ribofuranosyl-9*H*-purine **9** and the known *C(5′)-S*-acetate **10** [6] (*Scheme*). To obtain **9**, we debenzoylated the *C(8)*-substituted adenosine **4** [6] to the amine **5** (94%). Its reductive deamination with 3-methylbutyl nitrite in dry THF at 50° according to [22] provided **6** in yields of only 30–40% besides several by-products, of which the inosine **7** was isolated in *ca.* 5% yield. It presumably results from

substitution of the intermediate diazonium salt by H_2O generated upon diazotisation of **5**. The yield of **6** was indeed increased to 59% by batchwise addition of a tenfold excess of 3-methylbutyl nitrite to a 0.05M solution of **5** in dry THF and in the presence of activated 4-Å molecular sieves at 50°, although **7** was still formed. It was isolated in a yield of 12%, suggesting that the altered reaction conditions mostly suppressed its transformation into follow-up products, in agreement with the decreased amount and number of side-products. Detritylation of **6** with $Cl_2CHCOOH$ and Et_3SiH afforded the alcohol **8**. The alcohol was transformed into the chloride **9** (96%) by mesylation, completing the transformation of the intermediate methanesulfonate by adding 1 equiv. of LiCl. A solution of **9** and the *S*-acetate **10** in MeOH was treated with MeONa, resulting in *S*-deacetylation, nucleophilic substitution, and *N*-debenzoylation, and leading to the ^{H}A*[s]U dimer **11** that was desilylated with $(HF)_3 \cdot Et_3N$ to give the desired dinucleoside **3** in 95% yield.

Scheme

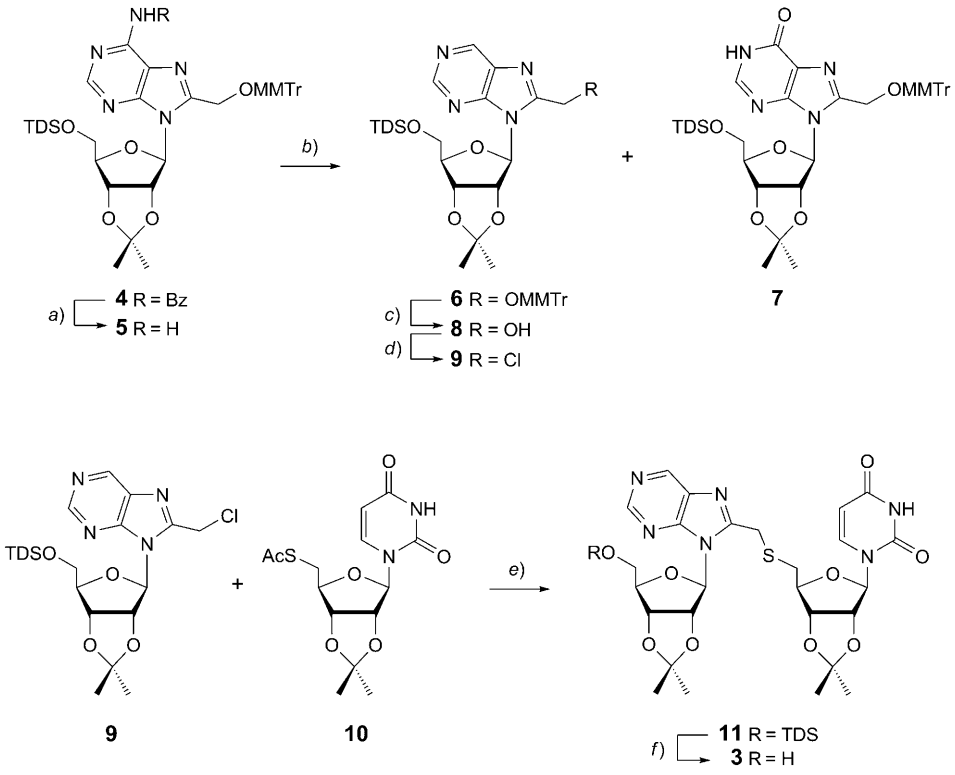

TDS = thexyl(dimethyl)silyl (= dimethyl(1,1,2-trimethylpropyl)silyl)
MMTr = (monomethoxy)trityl (= (4-methoxyphenyl)diphenylmethyl)

a) MeONa, MeOH, 0° to 25°; 94%. *b*) 3-Methylbutyl nitrite, THF, mol. sieves (4 Å), 50°; 59% of **6**, 12% of **7**. *c*) Et_3SiH, Cl_2CHCO_2H, CH_2Cl_2; 68%. *d*) MsCl, $EtN(i\text{-}Pr)_2$, CH_2Cl_2, 0° to 25°, then LiCl; 96%. *e*) MeONa, MeOH, 0° to 25°; 98%. *f*) $(HF)_3 \cdot Et_3N$, THF, 25°; 95%.

2. *Conformation of the Adenosine-Derived Monomers.* The purine nucleosides **5**, **6**, and **9** in $CDCl_3$ adopt a *syn*-conformation, as revealed by δ(H–C(2′)) of 5.81, 5.85, and 5.84 ppm, respectively (see *Table 1*). J(1′,2′)/J(3′,4′) of 0.74, 0.75, and 0.69, respectively, evidence a predominant *N* conformation. J(4′,5′a) and J(4′,5′b) values for **5** and **6** (6.2–6.7 Hz) agree with a *ca.* 1:1 *gt*/*tg* mixture, typical for S-linked dinucleosides [6], while **9** shows a higher proportion of the *gg*-rotamer (*gg*/*gt*/*tg* 23:36:41), as revealed by J(4′,5′a) and J(4′,5′b) values of 5.6 and 5.7 Hz, respectively[2]). The upfield shift for H–C(2′) (5.62 ppm) and the downfield for H–C(1′) (6.37 ppm) of **8**, as compared to **5**, **6**, and **9** (δ(H–C(1′)) = 6.19–6.32 ppm), reflect a *ca.* 4:1 *syn*/*anti* mixture (see [6]). Conceivably, an intramolecular H-bond between $HOCH_2$–C(8) (br. *s* at 4.70 ppm) and O–C(5′) decreases the destabilization of the *anti*-conformer by this CH_2OH group (*cf.* [6]). The interpretation is in keeping with J(4′,5′a) and J(4′,5′b) values of 5.0 Hz, evidencing a higher population of the *gg*-conformer of **8** (*gg*/*gt*/*tg* 36:30:34) than of **5**, **6** (*gt*/*tg* *ca.* 1:1), and **9** (*gg*/*gt*/*tg* 23:36:41). The ratio of the ribofuranose conformers of **8** is not affected by the intramolecular H-bond, as revealed by J(1′,2′)/J(3′,4′) = 0.71, similar to the ratio observed for **5**, **6**, and **9**.

Table 1. *Selected ^{1}H-NMR Chemical Shifts* [ppm] *and Coupling Constants* [Hz] *of the Adenosine-Derived Monomers* **5**–**9** *in $CDCl_3$*

	5	**6**	**7**	**8**	**9**
H–C(2)	8.29	8.96	8.05	8.92	8.96
H–C(6)	–	9.11	–	9.02	9.10
CH_a–C(8)	4.45	4.59	4.45	4.99	4.93
CH_b–C(8)	4.40	4.54	4.38	4.94	4.89
H–C(1′)	6.19	6.27	6.10	6.37	6.32
H–C(2′)	5.81	5.85	5.62	5.62	5.84
H–C(3′)	5.02	5.06	4.91	5.06	5.11
H–C(4′)	4.17	4.18	4.09	4.24	4.28
H_a–C(5′)	3.78	3.78	3.74	3.80	3.70
H_b–C(5′)	3.63	3.66	3.65	3.67	3.60
J(H_a,H_b)	11.8	11.8	11.5	14.7	12.7
J(1′,2′)	2.5	2.7	2.8	2.7	2.4
J(2′,3′)	6.5	6.6	6.7	6.6	6.4
J(3′,4′)	3.4	3.6	3.8	3.8	3.5
J(4′,5′a)	6.7	6.2	6.1	5.0	5.6
J(4′,5′b)	6.4	6.2	6.2	5.0	5.7
J(5′a,5′b)	11.8	10.7	10.7	11.0	10.9

The chemical shift for H–C(2′) of **7** (5.62 ppm) is lower than the one for **5** and **6**, while the *S*/*N* ratio of **7** is similar, as expressed by J(1′,2′)/J(3′,4′) = 0.74; also J(4′,5′a) and J(4′,5′b) values are similar (6.1–6.2, as compared to 6.2–6.7 Hz), revealing a *ca.* 1:1 *gt*/*tg* rotamer distribution. The upfield shift for H–C(2′) of **7** ($\Delta\delta$ 0.19–0.23 ppm), reflecting a different *syn*-conformation, or a higher proportion of the *anti*-conformer, shows a subtle influence of the nature of the nucleobase.

[2]) See [6] for the calculation of the rotamer distribution.

3. *Conformation and Association of the $^{H}A^{*}[s]U$ Dimers in $CHCl_3$.* The deaminated purine moiety in unit II of the $^{H}A^{*}[s]U$ dimers **11** and **3** cannot form *Watson–Crick*- or *Hoogsteen*-type H-bonds, while U·U base pairing [23] may lead to linear dimers, but not to higher associates. The conformation of unit I is similar for the two $^{H}A^{*}[s]U$ dimers **11** and **3**. The chemical shift for H–C(2′/I) of **11** and **3** (4.95 and 4.94 ppm, resp.; *Table 2*) is typical for a *ca.* 1:1 *syn*/*anti* orientation of the uracil moiety (see [6]). The predominant *N* conformation of the furanose ring of unit I of **11** and **3** is characterized by the same $J(1',2')/J(3',4')$ ratio of 0.49. $J(4',5'a = 6.3$ Hz) and $J(4',5'b = 6.4$ Hz) for unit I of **11**, and the similar values of 6.0 and 6.3 Hz for **3** evidence a *ca.* 20:40:40 and a *ca.* 24:38:38 *gg*/*gt*/*tg* equilibrium, respectively.

Table 2. *Selected ^{1}H-NMR Chemical Shifts* [ppm] *and Coupling Constants* [Hz] *of the $^{H}A^{*}[s]U$ Dimers* **11** *and* **3** *in $CDCl_3$*

	11 71 mM	**3** 26 mM		**11** 71 mM	**3** 26 mM
Uridine unit (I)			Adenosine-derived unit (II)		
H–N(3/I)	9.71	9.58	H–C(6/II)	9.06	9.10
H–C(1′/I)	5.59	5.58	H–C(2/II)	8.91	8.90
H–C(2′/I)	4.95	4.94	CH_a–C(8/II)	4.18	4.07
H–C(3′/I)	4.71	4.67	CH_b–C(8/II)	4.07	4.07
H–C(4′/I)	4.27	4.26	H–C(1′/II)	6.30	6.14
H_a–C(5′/I)	2.95	3.00	H–C(2′/II)	5.94	5.30
H_b–C(5′/I)	2.92	2.94	H–C(3′/II)	5.11	5.11
$J(1',2'/I)$	2.1	2.1	H–C(4′/II)	4.26	4.52
$J(2',3'/I)$	6.6	6.6	H_a–C(5′/II)	3.62	3.96
$J(3',4'/I)$	4.3	4.3	H_b–C(5′/II)	3.53	3.79
$J(4',5'a/I)$	6.3	6.0	$J(H_a,H_b/II)$	14.6	[a])
$J(4',5'b/I)$	6.4	6.3	$J(1',2'/II)$	2.1	5.0
$J(5'a,5'b/I)$	14.0	14.0	$J(2',3'/II)$	6.3	5.9
			$J(3',4'/II)$	3.2	1.6
			$J(4',5'a/II)$	6.2	2.0
			$J(4',5'b/II)$	6.1	2.3
			$J(5'a,5'b/II)$	10.7	12.8
			$J(HO,5'a/II)$	–	2.0
			$J(HO,5'b/II)$	–	11.0

[a]) Not assigned.

The nature of the substituent at C(5′/II) influences the conformation of unit II. The silyl ether **11** adopts a *syn* conformation, as revealed by $\delta(H–C(2'/II)) = 5.94$ ppm. A *ca.* 24:40:36 *gg*/*gt*/*tg* equilibrium is deduced from $J(4',5'a/II) = 6.2$ Hz and $J(4',5'b/II) = 6.1$ Hz. A $J(1',2'/II)/J(3',4'/II)$ ratio of 0.62 evidences a predominant *N* conformation. HO–C(5′/II) of **3** forms a persistent intramolecular H-bond to N(3), as evidenced by the dominant population of the *gg*-rotamer ($J(4',5'a/II) = 2.0$ Hz, $J(4',5'b/II) = 2.3$ Hz), the preferred *S* conformation of the furanose ($J(1',2')/J(3'/4') = 3.1$), the chemical shift of HO–C(5′/II) (5.61 ppm), the upfield shift of H–C(2′/II) (5.30 ppm), and the typical $J(5',OH)$ values of 2.0 and 11.0 Hz (*cf.* [2][6][24]).

The self-association of **11** and **3** was investigated by analysing the concentration dependence of the chemical shift for H–N(3/I). The ^{H}A*[s]U dimers **11** and **3** associate but weakly (K_{ass} = 23 and 20 M^{-1}, resp.) and form linear associates, as shown by the weak curvature of the shift/concentration curves (*SCC*; *Fig. 1*), the absence of a plateau at concentrations between 20 and 50 mM, and the numerical analysis according to the method of *Gutowsky* and *Saika* [25][6] (*Table 3*). As expected, the association constants for the ^{H}A*[s]U dimers **11** and **3** are slightly higher than those for 3′,5′-*O*-diacetyl-2′-deoxyuridine (12.7 M^{-1}) [26] and 1-cyclohexyluracil (3.2 M^{-1} [27] to 6.1 M^{-1} [28]), but an order of magnitude lower than those for self-complementary A*[s]U dimers (221–225 M^{-1}, see [6]).

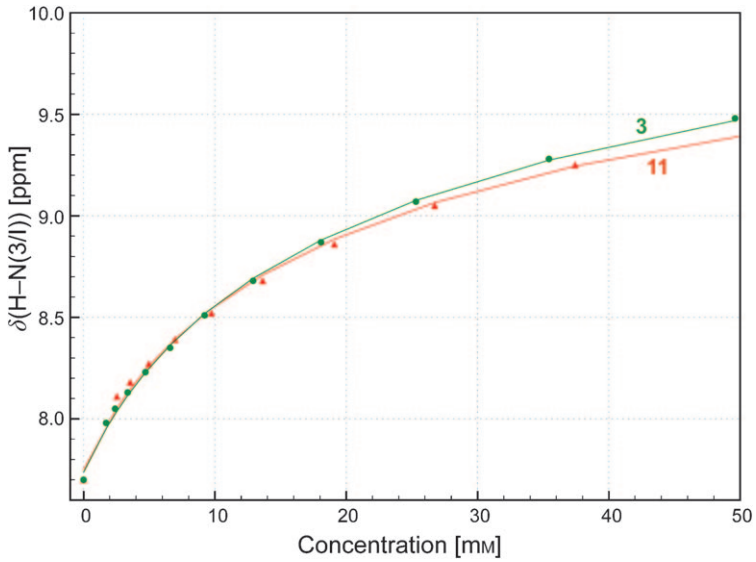

Fig. 1. *Shift/concentration curves* (SCCs) *for the ^{H}A*[s]U dimers* **11** *and* **3** *in $CDCl_3$ solution* (including a value of 7.70 ppm for a 0.0001-mM soln.)

Table 3. *Association Constants* K_{ass} *from the Concentration Dependence of δ(HN(3)) in $CDCl_3$ at 295 K for the ^{H}A[s]U Dimers* **11** *and* **3** (including a value of 7.70 ppm for a 0.0001-mM soln.), ΔG_{295} *Values, and Extrapolated Chemical Shifts of the Monoplexes and Duplexes*

Dimer	K_{ass} [M^{-1}]	$-\Delta G_{295}$ [a]) [kcal/mol]	$\delta_{monoplex}$ [b]) [ppm]	δ_{duplex} [c]) [ppm]
11	23	1.8	7.74	10.88
3	20	1.8	7.74	11.17

[a]) Calculated from K_{ass}. [b]) Extrapolated for 0 mM. [c]) Extrapolated for infinite concentration.

The weak self-association of **11** and **3** in $CHCl_3$ is also evidenced by the CD spectra, the molar ellipticity ([θ]) ranging from *ca.* $-5\cdot10^3$ to $+10^4$ deg·cm^2·dmol^{-1}, as compared to [θ] of the corresponding A*[s]U dimers, ranging from *ca.* $-6\cdot10^4$ to $+2\cdot$

10^4 deg · cm^2 · dmol^{-1} [6][3]). The CD spectra of 1 mM solutions of **11** and **3** in $CHCl_3$ in the temperature range of 0–50° (*Fig. 2*) show a weak variation of the ellipticity, in agreement with poor stacking, as expected for weakly associating species. Two positive *Cotton* effects around 270 and 245 nm are observed for **11**, whereas **3** shows a negative effect around 280 nm.

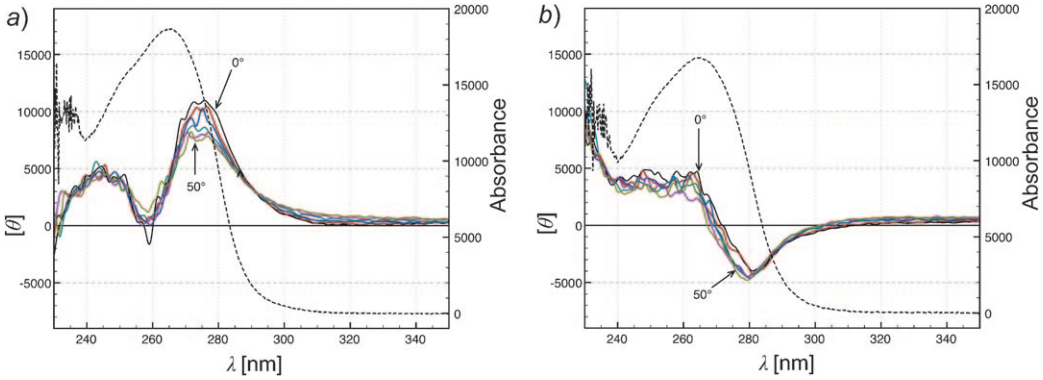

Fig. 2. *Temperature-dependent CD spectra* (solid lines, in 10° steps from 0° to 50°) *and UV spectra* (dashed lines) *of 1-*mM *solutions of* a) **11** *and* b) **3** *in* $CHCl_3$

4. *Characterization of the Gels.* 4.1. *Solvents.* We first evaluated the gelation of a selection of solvents by the A*[s]U$^{(*)}$ dimers **1** and **2**, and by the ^{H}A*[s]U dimer **3**. The selection is based on *Chastrette*'s classification of solvents into nine categories that agrees well with chemical intuition [29]. To overcome its limitations, we modified it by introducing a class of aliphatic apolar solvents, including solvents from an 'unexpected' class [29] and solvents that were not considered in the original classification, according to structural analogy. This resulted in the 33 solvents in *Table 4*.

The solubility of **1**, **2**, and **3** in the selected solvents, and the properties of the resulting gels were evaluated at a gelator concentration of 1% (*w*/*v*), considering the availability of the dinucleosides and the efficiency of other nucleobase-containing organogelators [8][30–33] (*Table 4*; see *Exper. Part* for details).

Inspection of *Table 4* shows that **3**, the deaminated analogue of **1**, does not form a gel with any of the solvents tested, while the A*[s]U dimer **1** forms partial gels[4]) in acetophenone, CH_2Cl_2, acetone, and $CHCl_3$, and clear or turbid gels in many of the aprotic dipolar and H-bonding solvents. Turbid gels presumably contain aggregates of a size comparable to the wavelength of visible light, whereas clear gels contain smaller aggregates [34]. The A*[s]U* dimer **2** is soluble in a larger number of solvents than **1**. While **1** forms gels in most of the alcohols tested, **2** is soluble in all of them. It forms partial gels in benzene, toluene, and CH_2Cl_2, and turbid gels in MeCN and AcOEt. In most solvents, **3** is about as soluble as **2**. No significant increase of the viscosity of the solutions of **3** was observed that could indicate the formation of associates.

---

[3]) For the sake of comparison, the ellipticity (θ [mdeg]) values reported in [6] were converted to [θ] [deg · cm^2 · dmol^{-1}].

[4]) See *Exper. Part* for a definition and evaluation of partial gels.

Table 4. *Solubility of the Dinucleosides* **1**, **2**, *and* **3** *in Selected Solvents, and Properties of the Gels*[a])

Class	Solvent	**1**	**2**	**3**
Aliphatic, apolar[b])	Pentane[b])	I[e])	I[e])	I[e])
	Hexane[c])	I	I	I
	Cyclohexane[c])	I	I	I
	CCl_4[c])	I	I	I
Aromatic, apolar	Benzene	I	PG	S
	Toluene	I	PG	I[g])
Aromatic, relatively polar	Acetophenone	PG[d])	S	S
Electron-pair donor	Et_2O	I[e])	I[e])	I[e])
	$(i\text{-Pr})_2O$	I	I	I
	t-BuOMe[b])	I	I	I
	1,4-Dioxane	S	S	S
Aprotic, dipolar	CH_2Cl_2	PG	PG	S
	Acetone	PG[f])	S	S
	$ClCH_2CH_2Cl$	**CG**	S	S
	Butan-2-one	**CG**	S	S
	MeCN	**CG**	**TG**	S
	AcOEt	**TG**	**TG**	S
Aprotic, highly dipolar	DMF	S	S	S
	DMSO	S	S	S
Aprotic, highly dipolar, and highly polarizable	Sulfolane	S	S	S
H-Bonding	2,2,2-Trifluoroethanol	S	S	S
	MeOH	S	S	S
	EtOH	**TG**	S	S
	PrOH	**TG**	S	S
	BuOH	**TG**	S	S
	Pentanol	**TG**	S	S
	Decanol[b])	**TG**	S	S
	i-PrOH	**TG**	S	S
	t-BuOH	**TG**	S	S
H-Bonding, strongly associated	H_2O	I	I	I
Miscellaneous	$CHCl_3$	PG	S	S
	1,2-Dimethoxyethane[c])	S[e])	S[e])	S[e])
	THF[c])	S[e])	S[e])	S[e])

[a]) [gelator] = 1% (*w*/*v*), I: insoluble, S: soluble, PG: partial gel, CG: clear gel, TG: turbid gel. [b]) Missing in *Chastrette*'s original classification [29]. [c]) Reclassified solvent. [d]) After 5 d. [e]) At 25°. [f]) After 36 h. [g]) Soluble at 70°.

The results in *Table 4* show the crucial role of the C(6)–NH_2 group of the adenosine moiety for the formation of gels, and evidence that H-bonding between the complementary nucleobases is the (or a) main driving force leading to a network of

the gelator, rather than just the interaction of the CH_2OH groups. These results and the tendency of the dinucleosides to form cyclic duplexes, as discussed in the preceding paper [6], suggest that gelation is the result of a subtle balance between the formation of cyclic and linear associates, considering that **2** shows a weaker tendency to form gels than **1**, but a stronger one to form cyclic duplexes [6]. Thus, **1** forms linear associates more readily than **2**, in agreement with the higher population of the *anti*-conformation of unit I in **1**. *anti*-Conformers indeed lead exclusively to linear associates, while a *syn*-conformation is required for the formation of cyclic duplexes [2][3][6].

4.2. *Gel–Sol Transition Temperature and Minimum Gelation Concentration.* The gel–sol transition (melting) temperature (T_m) of the gels formed by **1** and **2** depends strongly on the gelled solvent (*Table 5* and *Exper. Part*). The gels of **1** and $ClCH_2CH_2Cl$, butan-2-one, and MeCN exhibit T_m values of 62°, 58°, and 49° respectively, while a broad transition between *ca.* 62 and 75° was observed for the gel with AcOEt. T_m Values of the gels of **2**, and MeCN or AcOEt are 54° and 56°, respectively. T_m Values of the gels of **1** in linear alcohols increase with the length of the alkyl chain of the solvent, ranging from 50° in EtOH to 84° in decanol, whereas T_m of the branched i-PrOH and *t*-BuOH are 54° and 48°, respectively.

Table 5. *Gel–Sol Transition Temperature* (T_m) *of 1% (w/v) Gels of* **1** *and* **2**

Solvent		**1**	**2**
Aprotic dipolar solvents	$ClCH_2CH_2Cl$	62°	–
	Butan-2-one	58°	–
	MeCN	49°	54°
	AcOEt	62–75°	56°
H-Bonding solvents	EtOH	50°	–
	PrOH	52°	–
	BuOH	53°	–
	Pentanol	65°	–
	Decanol	84°	–
	i-PrOH	54°	–
	t-BuOH	48°	–

The minimum gelation concentration (MGC), *i.e.,* the minimum amount of **1** and **2** required to gel a given volume of solvent, varies significantly with the solvent (*Table 6* and *Exper. Part*). The lowest MGC for the gels of **1** in an aprotic dipolar solvent was observed for $ClCH_2CH_2Cl$ (0.4%), while gelation of butan-2-one, MeCN, and AcOEt requires 0.5, 0.6, and 0.8% of **1**, respectively. The MGC of **2** is 0.6% in MeCN and 0.9% in AcOEt, comparable to the MGC of **1**. Gelation of i-PrOH and *t*-BuOH required 0.4 and 0.6% of **1**, respectively. A regular decrease of the MGC of **1** from 0.8 to 0.3% was observed for linear alcohols from EtOH to decanol. The gelation efficiency of **1** and **2** in terms of MGC is similar to that of other nucleobase-containing gelators that gel alkanes at a concentration of *ca.* 0.3% [31][33], but lower than the one of trehalose esters which gel AcOEt [35], or of benzylidene derivatives of pyranosides that gel cyclohexane [36] at concentrations as low as 0.04%.

The variation of T_m and MGC for the gels of **1** in linear alcohols shows a strengthening of the self-association of the gelator with increasing length of the alkyl

Table 6. *Minimum Gelation Concentration* (MGC) *of the Gels of* **1** *and* **2**

Solvent		**1** (*w*/*v*)	**2** (*w*/*v*)
Aprotic dipolar solvents	$ClCH_2CH_2Cl$	0.4%	–
	Butan-2-one	0.5%	–
	MeCN	0.6%	0.6%
	AcOEt	0.8%	0.9%
H-Bonding solvents	EtOH	0.8%	–
	PrOH	0.7%	–
	BuOH	0.6%	–
	Pentanol	0.5%	–
	Decanol	0.3%	–
	i-PrOH	0.4%	–
	t-BuOH	0.6%	–

chain of the solvent, the gel of **1** and decanol exhibiting the lowest MGC and the highest T_m. Conversely, the gel of **1** and EtOH exhibits the highest MGC and the lowest T_m. In a series of homologous linear alcohols, the elongation of the alkyl chain affects mainly the polarity of the bulk solvent. *Zhu* and *Dordick* reported a correlation between the gelation number (related to MGC) of trehalose diester gels and the polarity parameter $E_T(30)$ [37], the most comprehensive empirical solvent polarity scale known so far [38][39]. Similarly, the MGC for the gels of **1** and linear alcohols increases with the increasing polarity parameter E_T^N of the solvent, while T_m decreases (*Fig. 3*). This is in agreement with the observation that H-bonding is the main force responsible for the association of the gelator, as highly polar solvents weaken H-bonds to a greater extent than less polar ones. The trend followed by gels in i-PrOH and *t*-BuOH (not shown) is different, evidencing that the constitution of the alcohols affects the association of the gelator, independently of the polarity of the solvent.

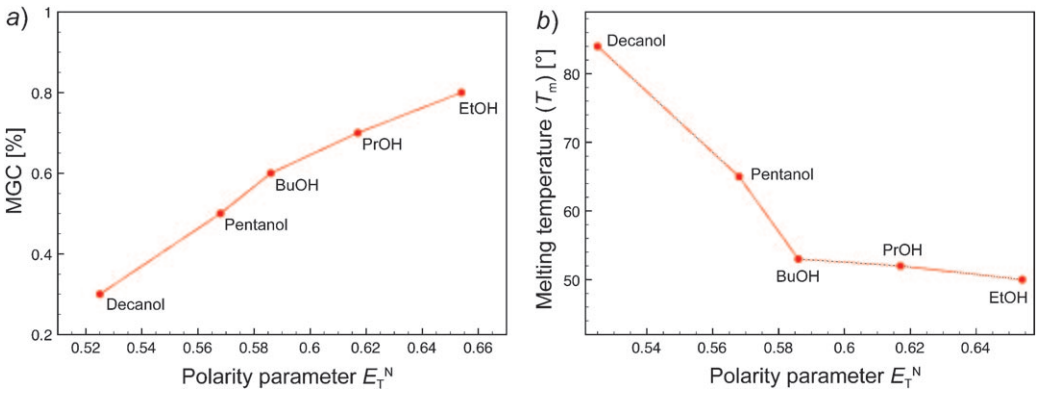

Fig. 3. *Effect of the polarity parameter* E_T^N *of the solvents on* a) *MGC and* b) T_m *of the gels of* **1**. E_T^N Values are taken from [39].

4.3. *Rheological Characterization.* The rheological properties of some of the gels of **1** and **2** were evaluated by amplitude and temperature sweeps [40].

Amplitude Sweeps. The variation of the storage modulus (G'), related to the elastic behaviour of the sample, and of the loss modulus (G''), related to the viscous behaviour, were determined for gels formed by 1% (*w*/*v*) of **1** in $ClCH_2CH_2Cl$, MeCN, AcOEt, EtOH, pentanol, and decanol as a function of increasing and decreasing strain at a constant temperature and frequency (*Fig. 4*; see *Exper. Part*).

For all gels of **1** studied, the elastic behaviour dominated over the viscous one at low amplitudes ($G' > G''$), revealing the rigidity of the gel, *i.e.,* a solid-like behaviour. Moreover, each one of the functions $G'(\gamma)$ and $G''(\gamma)$ [41] showed a constant plateau value below the limit of the linear viscoelastic (LVE) range [41], showing that the structure of the gel is stable under low-deformation conditions. At amplitudes higher than the limit of the LVE range (γ_L), the structure of the gel started to change irreversibly [41]; for **1**, the γ_L values ranged between 0.3% in MeCN, and 0.6% in EtOH and decanol. As the amplitude increased further, the viscous behaviour started to dominate over the elastic one ($G'' > G'$), and the sample exhibited a liquid character. Depending on the solvent, the gel–sol transitions occurred at strain values ranging from 3 to 9%. The reversibility of the gelation was evidenced by a sweep with decreasing amplitudes. As the strain exerted on a liquid mixture of gelator **1** and solvent ($G'' > G'$) decreased, the elastic behaviour increased more rapidly than the viscous one, and the gel character of the sample ($G' > G''$) was fully recovered at strain values ranging from 0.5 to 3%.

Similar oscillatory tests of gels formed by 1% (*w*/*v*) of **2** in MeCN and AcOEt (*Fig. 5*) also evidenced the domination of the elastic over the viscous behaviour ($G' > G''$). In contradistinction to the gels formed from **1**, neither the function $G'(\gamma)$ nor $G''(\gamma)$ showed a constant value upon increasing the strain from 0.1 to 100%, evidencing a low γ_L value ($< 0.1\%$). The gel of **2** and MeCN exhibited a gel–sol transition at a strain of *ca.* 2%, while the sol–gel transition of the gel formed with AcOEt required a significantly higher strain (*ca.* 30%). Reversible gelation was observed upon decreasing the amplitude, reconstitution of the gel occurring at a strain of *ca.* 0.3% for **2** in MeCN and *ca.* 10% for **2** in AcOEt.

The significantly lower γ_L values observed for gels derived from **2** as compared to those derived from **1** indicate that the former are less resistant to strain than the latter *i.e.,* that the strength of the inter-gelator association is weaker for **2** than for **1**, in keeping with the interpretation of the gel-forming tendency of these dinucleosides.

Temperature Sweeps. We only investigated the temperature effect on the dynamic moduli G' and G'' for the gels of **1** (*Fig. 6*; see *Exper. Part*), considering the low γ_L values for the gels of **2**. The domination of the storage modulus of the gels of **1** and $ClCH_2CH_2Cl$, MeCN, EtOH, pentanol, and decanol over the loss modulus ($G' > G''$, gel character) was observed for a rather wide range of temperatures, up to the melting temperature (T_m) where the viscous behaviour became predominant ($G'' > G'$). The agreement between the gel–sol transition temperatures determined by this technique and by visual inspection was satisfactory (*Table 5*; 40° *vs.* 49° for MeCN, 53° *vs.* 50° for EtOH, 65° *vs.* 65° for pentanol, 87° *vs.* 84° for decanol), with the exception for the gel with $ClCH_2CH_2Cl$ (78° *vs.* 62°). The difference observed for the gel with $ClCH_2CH_2Cl$ illustrates the difficulty of visual discrimination between a gel and a viscous solution. In addition, no crossing of the curves related to the temperature dependence of G' and G''

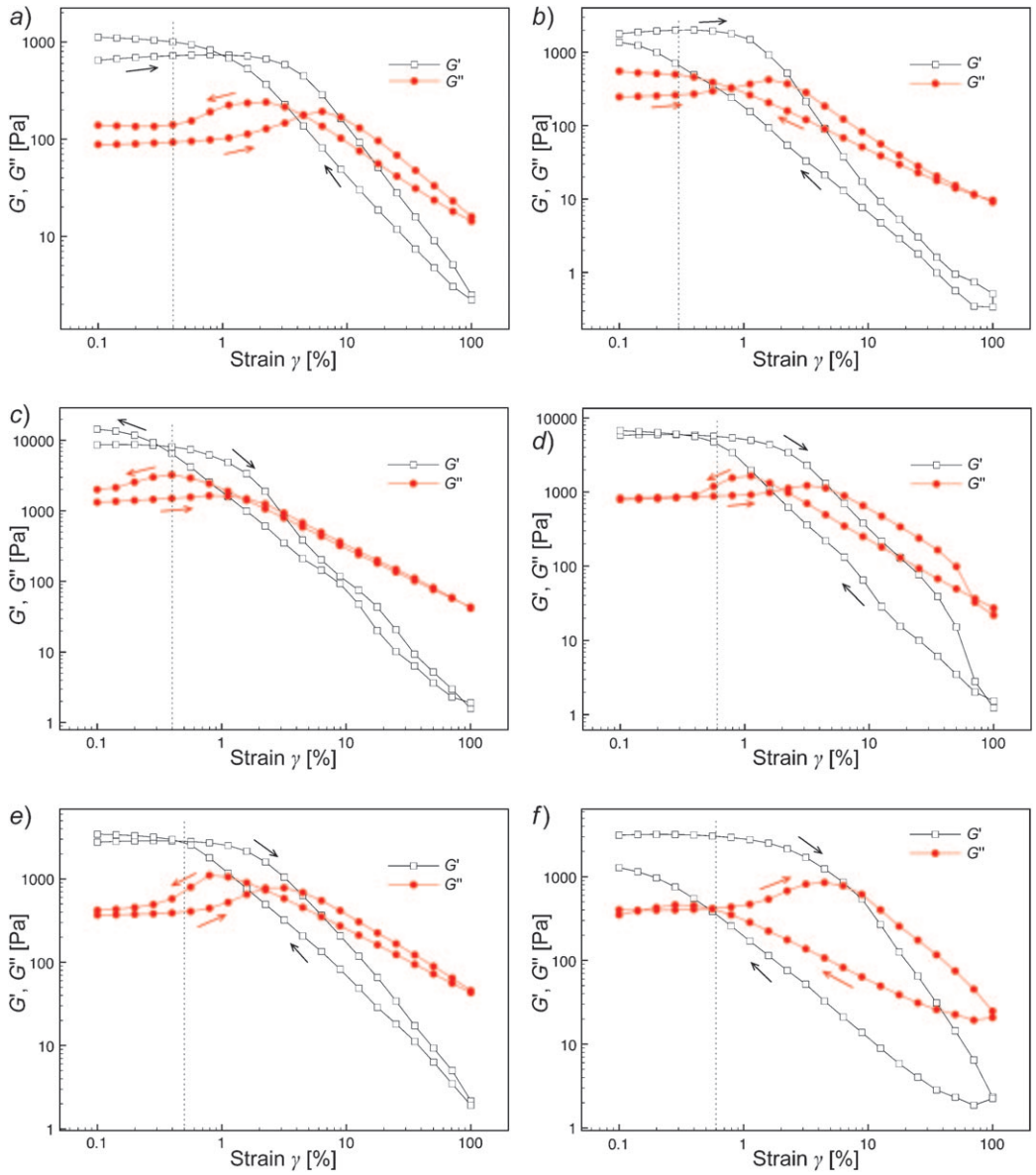

Fig. 4. *Amplitude sweep – variation of the storage* (G') *and loss* (G'') *moduli with increasing and decreasing strains for the 1% (w/v) gels of* **1** *in* a) $ClCH_2CH_2Cl$, b) *MeCN,* c) *AcOEt,* d) *EtOH*, e) *pentanol, and* f) *decanol at 25°*. The dotted lines represent the limit of the linear viscoelastic range (γ_L).

could be observed for the gel of **1** and AcOEt, in parallel to a broad gel–sol transition temperature.

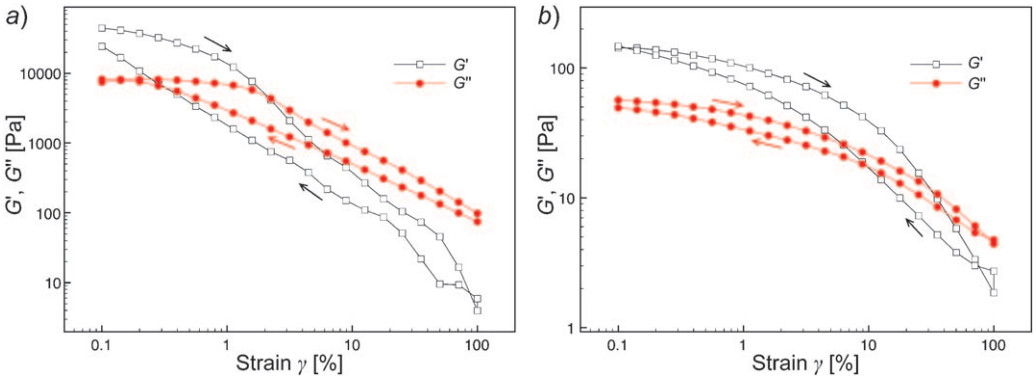

Fig. 5. *Amplitude sweep – variation of the storage* (*G′*) *and loss* (*G″*) *moduli with increasing and decreasing strains for the 1%* (*w*/*v*) *gels of* **2** *in* a) *MeCN and* b) *AcOEt at 25°*

4.4. *Circular Dichroism.* Temperature-dependent CD spectra of the gels formed by 1% (*w*/*v*) of **1** and $ClCH_2CH_2Cl$, MeCN, AcOEt, EtOH, PrOH, pentanol, and decanol, and of the gels of **2** in MeCN and AcOEt were measured to characterize their supramolecular structure [42]. Due to the relatively high concentration (*ca.* 16 mM) required for gelation as compared to the range of concentrations usually employed for CD studies, we modified the acquisition parameters (see *Exper. Part*). In contradistinction to the CD spectra of 1-mM solutions of A*[s]U(*) dinucleosides in $CHCl_3$ [6] which show extrema between *ca.* 260 and 280 nm, and no bands above 300 nm, the gels of **1** and **2** (*ca.* 16 mM) show intense CD signals between *ca.* 275 and 400 nm, and a weak signal to noise ratio below *ca.* 275 nm, due to the strong absorbance of the samples. Shape and intensity of the bands depend on the gelator and the solvent (*cf. Figs. 7* and *8*).

At 0°, the CD spectrum of the gel of **1** and MeCN shows a broad minimum around 315 nm, a maximum at *ca.* 300 nm, and a minimum at *ca.* 280 nm (*Fig. 7*). Increasing the temperature to 30° lowered the intensity of the minimum at *ca.* 315 nm, while the intensity of the extrema at *ca.* 300 and at *ca.* 280 nm increased. Further increasing the temperature to 40° resulted in a decrease of the intensity of the minimum around 315 nm, a slight increase of the intensity of the maximum at *ca.* 300 nm, and a decrease of the intensity of the minimum at *ca.* 280 nm. At 50°, above T_m of the gel, the CD bands could hardly be observed, evidencing a significantly lower degree of organisation.

The CD spectra of the gels of **1** and AcOEt, EtOH, PrOH (not shown), pentanol, and decanol exhibit a similar shape with a broad minimum around 310 nm (315 nm for decanol) and a maximum at *ca.* 290 nm (295 nm for decanol), but differ strongly from the CD spectra of **1** in MeCN. The temperature-dependent CD spectra of these gels exhibit isodichroic points at *ca.* 300 nm, and showed a regular decrease of intensity of the bands with increasing temperature. This suggests an equilibrium between two species, conceivably a weakly and a highly organised aggregate corresponding to weak and strong CD signals, respectively.

The CD spectra of the gel of **1** and $ClCH_2CH_2Cl$ were not reproducible, as the shape of the CD curve for a given sample depended on the orientation of the cell relative to the axis of the light beam, evidencing birefringency of the gel [42].

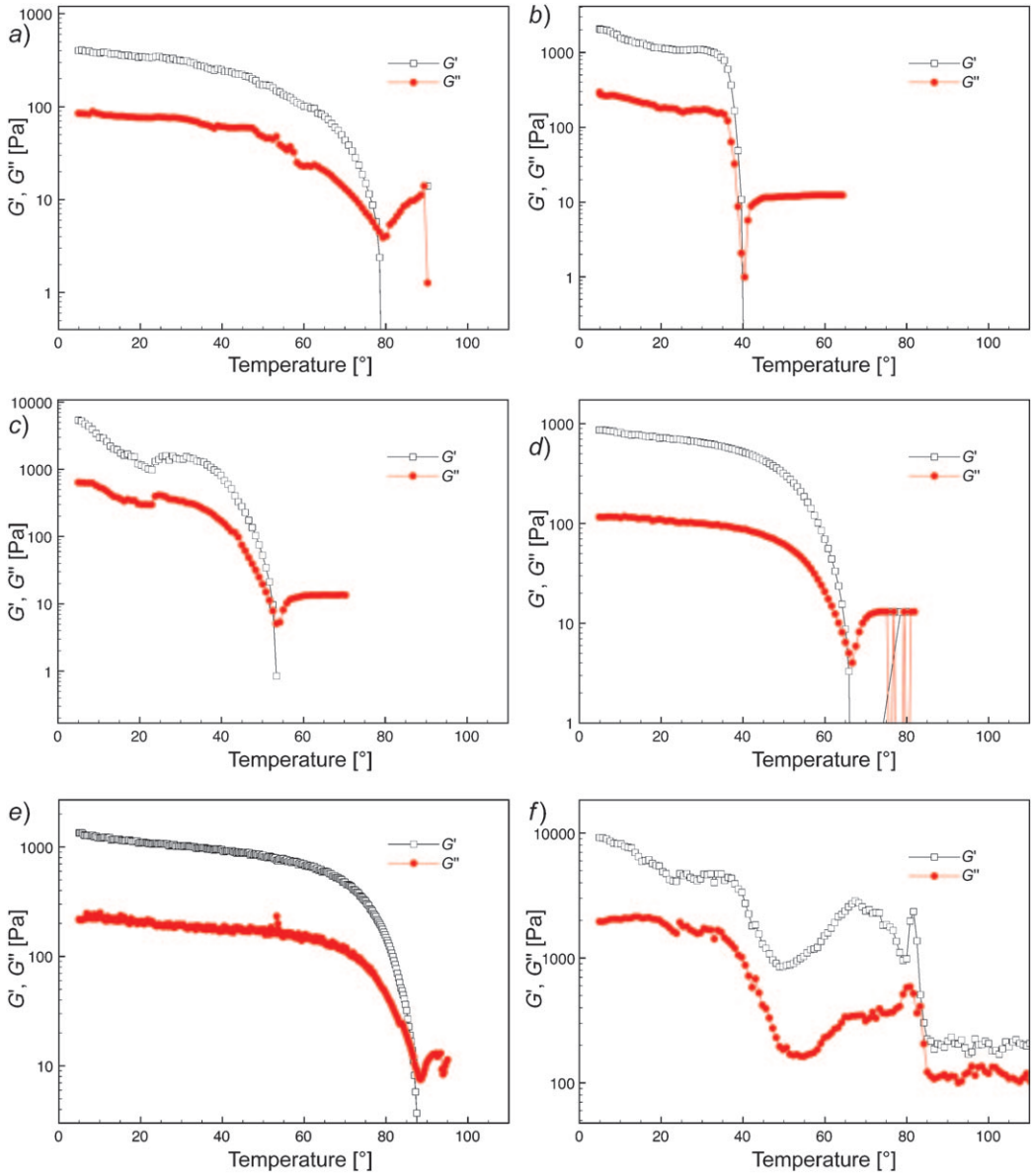

Fig. 6. *Temperature sweep – variation of the storage* (*G'*) *and loss* (*G''*) *moduli with increasing temperature for the 1%* (*w*/*v*) *gels of* **1** *in* a) $ClCH_2CH_2Cl$, b) *MeCN*, c) *EtOH*, d) *pentanol*, e) *decanol, and* f) *AcOEt at constant strain* (0.3%) *and frequency* (1 Hz)

The CD spectrum of the gel of **2** and MeCN at 0° shows a positive *Cotton* effect, with a broad maximum at *ca.* 300 nm and a minimum at *ca.* 285 nm. The intensity of the bands decreased steadily with increasing temperature (*Fig. 8*). The CD spectrum of the

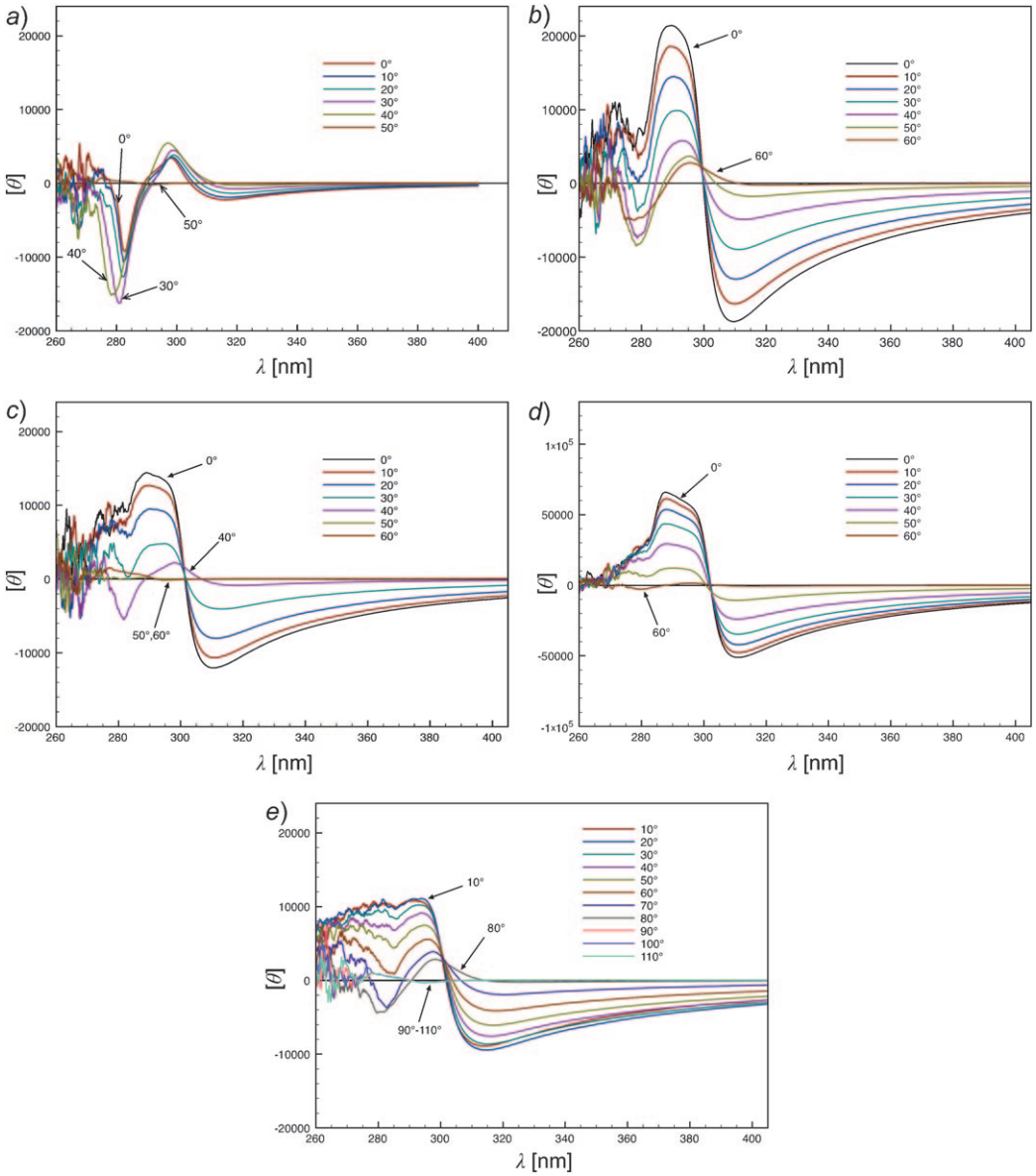

Fig. 7. *Temperature-dependent CD spectra of the 1% (w/v) gels of* **1** (16 mM) *in* a) *MeCN,* b) *AcOEt,* c) *EtOH,* d) *pentanol, and* e) *decanol*

gel of **2** and AcOEt at 0° shows a negative *Cotton* effect with a strong sharp minimum at *ca.* 295 nm, and a similar maximum at *ca.* 280 nm. Although no significant changes of intensity could be observed upon heating to 40°, increasing the temperature stepwise to 60°, above the T_m of the gel (54°), resulted in a decrease of the molar ellipticity. For

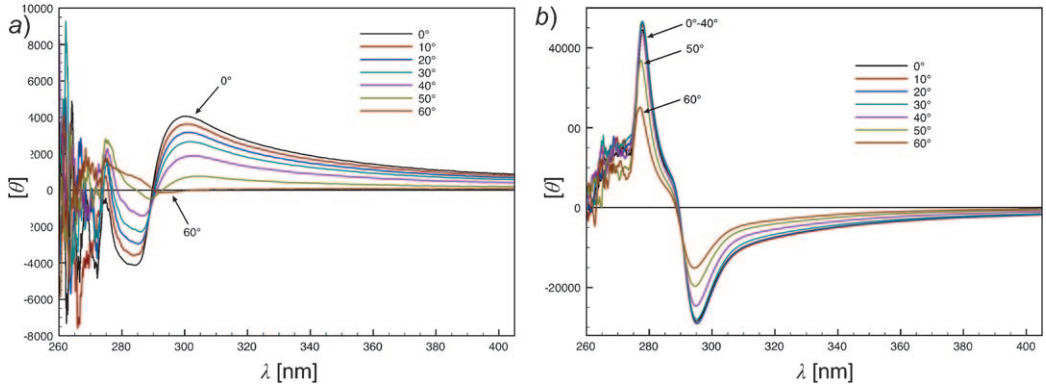

Fig. 8. *Temperature-dependent CD spectra of the 1% (w/v) gels of* **2** (15 mM) *in* a) *MeCN and* b) *AcOEt*

these two gels, we observed isodichroic points at *ca.* 290 nm, suggesting an equilibrium between a highly and a weakly organised aggregate of **2**, similarly as it was observed for the gels of **1**.

An intriguing feature of all CD spectra of the gels of **1** and **2** are strong bands with long tails above 300 nm. CD Bands at such wavelengths can hardly be the consequence of a red shift of the $\pi-\pi^*$ transition of the nucleobases. The maximal absorbance of the gels, too intense to be determined precisely, was found around 260 nm, typical for the $\pi-\pi^*$ transitions of uracil and adenine [43][44]. Cholesteric or chiral smectic C phases that may be formed upon gelation could give rise to CD signals outside the absorption region of the chromophore [42]. However, the formation of such liquid-crystalline phases was excluded upon inspecting the samples under polarized light in a microscope.

An extremum at 280 nm in the CD spectra of polyriboadenylic acids was reported by *Bush* and *Scheraga* [45] who suggested that it is due to a $n-\pi^*$ transition. That this band is absent in the CD spectra of mono- or dinucleotides is ascribed to solvation of the adenine ring and a blue shift of the $n-\pi^*$ band. Another example of a long-wavelength CD band around 295 nm was reported for stacked 6-*N*-methylated adenylyluridine [46] that exhibited a large CD effect as compared to the UV absorption, corroborating the $n-\pi^*$ character of the transition. The CD bands observed above 275 nm for the gels of **1** and **2** are thus likely to arise from a $n-\pi^*$ transition, and their intensity is expected to increase with the degree of association (and stacking) of the gelator.

Broad tail-shaped bands at longer wavelength were also observed for carotenoid aggregates [47] and ascribed to non-packed head-to-tail assemblies. Conceivably, the broad tail-shaped bands characterizing the CD spectra of the gels of **1** and **2** could also originate from non-packed aggregates that would slowly form a more tightly organized aggregate. The intensity of the broad tail-shaped bands is expected to decrease with aging of the gel. To test these hypotheses, we studied the influence of the gelator concentration and of aging the gel on the CD spectra (*cf. Fig. 9* and *10*).

The CD spectrum of a 0.3% solution of **1** in MeCN shows only a weak negative band at *ca.* 290 nm (*Fig. 9*). Increasing the concentration of **1** to 0.6% resulted in gelation of the solvent, and a broad negative CD band around 320 nm, a positive one

around 295 nm, and a negative one at *ca.* 280 nm. Further increasing the concentration of **1** to 1% has no effect on the negative tail-shaped band at *ca.* 320 nm, while the positive band was slightly red-shifted to *ca.* 300 nm, and the intensity of the negative band around 280 nm increased. This evidences the relation between the degree of association of the gelator and the apparition of CD signals above 300 nm. Conceivably, at a low concentration of **1**, the gelator–gelator interactions are weak, and the nucleobases solvated. This would result in a blue shift of the n–π^* transition band (*vide supra*). As the concentration of **1** increases, gelation of the solvent occurs, and a network of the gelator is formed. This requires desolvating the nucleobases, and results in a red shift of the n–π^* transition, occurring around 300 nm.

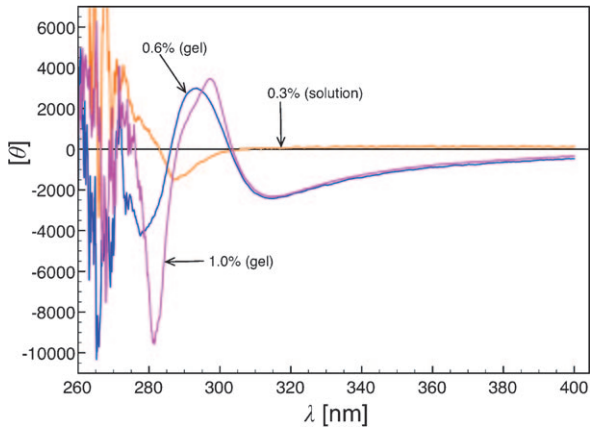

Fig. 9. *CD Spectra of the 0.3%* (*w*/*v*; solution), *0.6%* (*w*/*v*; gel), *and 1%* (*w*/*v*; gel) *mixtures of* **1** *and MeCN at 20°, recorded 1 h after gelation*

The CD spectrum of the 1% (*w*/*v*) gel of **1** and MeCN recorded 10 min after gel formation shows a broad negative, a positive, and a sharp negative band at *ca.* 320, 300, and 280 nm, respectively (*Fig. 10*). As the gel aged, the intensity of the broad tail-shaped negative band around 320 nm decreased. The intensity of the positive band at *ca.* 300 nm decreased slightly, while the band at *ca.* 280 nm was not affected. After 27 h, the CD spectrum remained unchanged. This suggests a slow rearrangement of the network of the gelator, as revealed by the decrease of the intensity of the broad tail-shaped band above 300 nm that may originate from tightly packed aggregates of the gelator.

We thank the *Swiss National Science Foundation* and *Syngenta AG*, Basel, for generous support.

Experimental Part

General. THF was distilled from Na/benzophenone, CH_2Cl_2, MeOH, DMF, pyridine, EtN(i-Pr)$_2$, and (i-Pr)$_2$NH from CaH_2. Reactions were run under N_2. Qual. TLC: precoated silica-gel plates (*Merck* silica gel *60 F254*); detection by spraying 'anisaldehyde' (EtOH (425 ml), AcOH (5 ml), H_2SO_4 (16 ml), *p*-anisaldehyde (10 ml)). Flash chromatography (FC): silica gel *Fluka 60* (0.04–0.063 mm). Optical rotations: 1-dm cell at 25° and 589 nm. Temp.-dependent CD (10° steps from 0° to 50°): 1-mM solns. in $CHCl_3$ in a 1-mm *Suprasil* cell. UV Spectra: 10^{-5} M solns. in $CHCl_3$ at 20° in a 1-cm *Suprasil* cell. FT-IR:

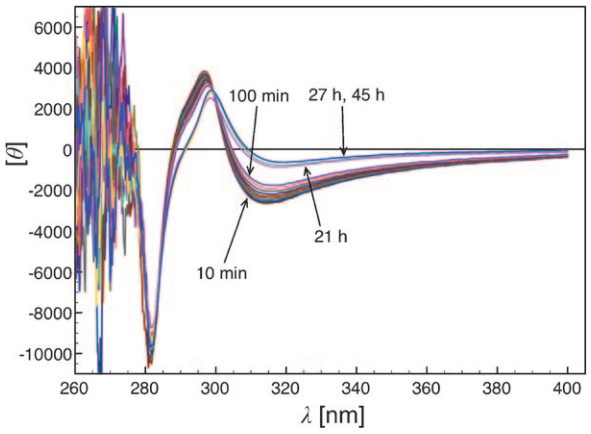

Fig. 10. *Time-dependent CD spectra of the 1%* (*w*/*v*; 16 mM) *gel of* **1** *and MeCN at 20°*

solid state (ATR). ^{1}H- and ^{13}C-NMR: at 300 or 400 MHz, and 75 or 100 MHz, resp. MS: matrix-assisted laser desorption ionization time-of-flight mass spectrometry (MALDI-TOF) with 0.05M indol-3-acrylic acid (IAA) in THF, or with 0.05M α-cyano-4-hydroxycinnamic acid (CCA) in MeCN/EtOH/H_2O, and high-resolution (HR) MALDI-TOF with 0.05M 2,5-dihydrobenzoic acid (DHB) in THF.

NMR Studies. NMR Experiments were performed at 295 K and at 300 MHz in $CDCl_3$ (passed through basic aluminium oxide and dried over mol. sieves (4 Å) prior to use). Experiments started at the highest concentration, with stepwise replacement of 225 µl of the 700 µl soln. with 225 µl of $CDCl_3$. The data were analysed by non-linear least-squares fitting using MATLAB (trust-region algorithm); the parameters were K_{ass}, δ(H–N(3), $c = 0$ mM), and δ(H–N(3), $c = \infty$).

*5′-*O*-[Dimethyl(1,1,2-trimethylpropyl)silyl]-2′,3′-*O*-isopropylidene-8-{[(4-methoxyphenyl)(diphenyl)methoxy]methyl}adenosine* (**5**). A soln. of **4** [6] (4.117 g, 4.88 mmol) in dry MeOH (12 ml) was cooled to 0°, treated with a freshly prepared 1.22M soln. of MeONa in MeOH (12.0 ml, 14.65 mmol) and stirred at 25° for 15 h. The mixture was cooled to 0°, and treated with sat. aq. NH_4Cl soln. (20 ml). After evaporation of MeOH, the residue was extracted three times with AcOEt. The combined org. layers were dried (Na_2SO_4) and evaporated. FC (cyclohexane/AcOEt 4:1 → 2:1 → 1:1) gave **5** (3.459 g, 94%). White solid. R_f (cyclohexane/AcOEt 1:2) 0.24. M.p. 84–88°. $[\alpha]_D^{25} = -201.9$ ($c = 0.075$, $CHCl_3$). UV ($CHCl_3$): 263 (40470). IR (ATR): 3464*w*, 3316*w*, 3157*w*, 2955*w*, 2867*w*, 1735*w*, 1638*m*, 1604*m*, 1578*w*, 1509*m*, 1490*w*, 1463*w*, 1446*m*, 1415*w*, 1373*m*, 1328*m*, 1298*m*, 1250*s*, 1213*m*, 1170*m*, 1154*m*, 1061*s*, 1034*s*, 976*m*, 932*w*, 900*w*, 869*m*, 830*s*. ^{1}H-NMR (300 MHz, $CDCl_3$): see *Table 1*; additionally, 7.55–7.22 (*m*, 12 arom. H); 6.88–6.83 (*m*, 2 arom. H); 6.04 (br. *s*, NH_2); 3.78 (*s*, MeO); 1.57 (*sept.*, $J = 6.9$, Me_2CH); 1.50, 1.38 (2*s*, Me_2C); 0.85, 0.82 (2*s*, Me_2CSi); 0.79 (*d*, $J = 6.9$, Me_2CH); 0.00, −0.02 (2*s*, Me_2Si). ^{13}C-NMR (75 MHz, $CDCl_3$): see *Table 7*; additionally, 158.94 (*s*); 143.67, 143.62 (2*s*); 134.70 (*s*); 130.61 (2*d*); 128.56 (4*d*); 128.13 (4*d*); 127.32 (2*d*); 113.97 (*s*, Me_2C); 113.44 (2*d*); 87.93 (*s*, Ph_2C); 55.31 (*q*, MeO); 34.19 (*d*, Me_2CH); 27.37, 25.73 (2*q*, Me_2C); 25.32 (*s*, Me_2CSi); 20.39 (*q*, Me_2CSi); 18.58, 18.55 (2*q*, Me_2CH); −3.30, −3.34 (2*q*, Me_2Si). HR-MALDI-MS: 752.3841 ($[M + H]^+$, $C_{42}H_{54}N_5O_6Si^+$; calc. 752.3838).

Reductive Deamination of **5**. A mixture of **5** (2.241 g, 2.98 mmol) and 4-Å mol. sieves (3 g) in dry THF (60 ml) was heated to 50°, treated hourly for 4 h with 3-methylbutyl nitrite (4 × 4 ml, 120 mmol), and evaporated. FC (cyclohexane/AcOEt 2:1 → 0:1) gave **6** (1.297 g, 59%) and **7** (274 mg, 12%). A sample of **7** for analysis was recrystallized in MeCN/$CHCl_3$ (*ca.* 100:1).

*Data of 5′-*O*-[Dimethyl(1,1,2-trimethylpropyl)silyl]-2′,3′-*O*-isopropylidene-8-{[(4-methoxyphenyl)-(diphenyl)methoxy]methyl}-β-*D*-ribofuranosyl-9*H*-purine* (**6**). White solid. R_f (cyclohexane/AcOEt 1:2) 0.53. M.p. 55–58°. $[\alpha]_D^{25} = -23.2$ ($c = 0.07$, $CHCl_3$). UV ($CHCl_3$): 267 (12990). IR (ATR): 3057*w*, 2956*w*, 2867*w*, 1727*w*, 1600*m*, 1584*w*, 1509*m*, 1491*w*, 1456*w*, 1448*w*, 1427*w*, 1372*w*, 1355*w*, 1300*w*, 1250*s*, 1213*m*, 1179*m*, 1154*m*, 1066*s*, 1034*s*, 974*m*, 916*w*, 901*w*, 870*w*, 830*s*. ^{1}H-NMR (300 MHz, $CDCl_3$): see *Table 1*; additionally, 7.57–7.24 (*m*, 12 arom. H); 6.91–6.85 (*m*, 2 arom. H); 3.81 (*s*, MeO); 1.58 (*sept.*, $J = 6.9$,

Table 7. *Selected ^{13}C-NMR Chemical Shifts* [ppm] *of the Adenosine-Derived Monomers* **5**–**9** *in $CDCl_3$*

	5	**6**	**7**	**8**	**9**
C(2)	152.77	152.38	144.27	152.63	153.10
C(4)	149.33	152.08	158.96[a])	152.24	151.98[a])
C(5)	119.07	133.69	124.46	132.90	133.31
C(6)	155.48	148.44	159.25[a])	148.03	149.12
C(8)	150.68	154.42	149.33[b])	156.81	152.53[a])
CH_2–C(8)	59.48	59.67	59.19	58.27	36.76
C(1′)	90.38	90.29	90.30	89.80	90.16
C(2′)	82.35	82.71	83.22	83.63	83.00
C(3′)	83.00	81.97	81.86	80.87	81.46
C(4′)	87.31	87.02	86.93	86.83	87.45
C(5′)	63.22	63.05	63.17	62.69	62.73

[a]) Assignment may be interchanged. [b]) May be interchanged with 149.67 ppm (see *Exper. Part*).

Me_2CH); 1.52, 1.40 (2*s*, Me_2C); 0.85 (*d*, *J* = 6.9, Me_2CH); 0.81, 0.80 (2*s*, Me_2CSi); 0.00 (*s*, Me_2Si). ^{13}C-NMR (75 MHz, $CDCl_3$): see *Table 7*; additionally, 158.99 (*s*); 143.47, 143.42 (2*s*); 134.44 (*s*); 130.62 (2*d*); 128.49 (4*d*); 128.16 (4*d*); 127.37 (2*d*); 114.29 (*s*, Me_2C); 113.48 (2*d*); 88.19 (*s*, Ph_2C); 55.32 (*q*, MeO); 34.16 (*d*, Me_2CH); 27.37, 25.68 (2*q*, Me_2C); 25.32 (*s*, Me_2CSi); 20.36 (*q*, Me_2CSi); 18.56, 18.54 (2*q*, Me_2CH); −3.36, −3.38 (2*q*, Me_2Si). HR-MALDI-MS: 737.3736 ($[M+H]^+$, $C_{42}H_{53}N_4O_6Si^+$; calc. 737.3729). Anal. calc. for $C_{42}H_{52}N_4O_6Si$ (736.98): C 68.45, H 7.11, N 7.60; found: C 68.23, H 7.12, N 7.47.

*Data of 5′-*O*-[Dimethyl(1,1,2-trimethylpropyl)silyl]-2′,3′-*O*-isopropylidene-8-{[(4-methoxyphenyl)-(diphenyl)methoxy]methyl}inosine* (**7**). White solid. R_f (cyclohexane/AcOEt 1:1) 0.29. M.p. 206°. $[\alpha]_D^{25} = -18.5$ (*c* = 0.93, $CHCl_3$). UV ($CHCl_3$): 246 (20230), 255 (sh, 18040), 276 (sh, 8990). IR (ATR): 3098*w*, 3055*w*, 2956*w*, 2867*w*, 1707*s*, 1607*w*, 1589*w*, 1555*w*, 1528*w*, 1509*m*, 1491*w*, 1460*w*, 1446*m*, 1375*w*, 1345*w*, 1298*w*, 1251*m*, 1212*m*, 1176*w*, 1155*w*, 1086*s* (sh), 1061*s*, 1034*s*, 983*w*, 970*w*, 931*w*, 900*w*, 862*m*, 828*s*. ^{1}H-NMR (300 MHz, $CDCl_3$): see *Table 1*; additionally, 13.05 (br. *s*, NH); 7.53–7.21 (*m*, 12 arom. H); 6.88–6.83 (*m*, 2 arom. H); 3.80 (*s*, MeO); 1.57 (*sept.*, *J* = 6.9, Me_2CH); 1.48, 1.36 (2*s*, Me_2C); 0.83 (*d*, *J* = 6.9, Me_2CH); 0.80, 0.79 (2*s*, Me_2CSi); 0.00 (*s*, Me_2Si). ^{13}C-NMR (75 MHz, $CDCl_3$): see *Table 7*; additionally, 149.67 (*s*); 143.68, 143.58 (2*s*); 134.73 (*s*); 130.66 (2*d*); 128.63 (4*d*); 128.14 (4*d*); 127.30 (2*d*); 114.46 (*s*, Me_2C); 113.50 (2*d*); 87.87 (*s*, Ph_2C); 55.38 (*q*, MeO); 34.25 (*d*, Me_2CH); 27.41, 25.72 (2*q*, Me_2C); 25.41 (*s*, Me_2CSi); 20.45 (*q*, Me_2CSi); 18.62 (*q*, Me_2CH); −3.23, −3.26 (2*q*, Me_2Si). HR-MALDI-MS: 775.3501 ($[M+Na]^+$, $C_{42}H_{52}N_4NaO_7Si^+$; calc. 775.3503). Anal. calc. for $(C_{42}H_{52}N_4O_7Si)\cdot 0.5\ H_2O$ (761.98): C 66.20, H 7.01, N 7.35; found: C 66.11, H 6.89, N 7.37.

*5′-*O*-[Dimethyl(1,1,2-trimethylpropyl)silyl]-8-(hydroxymethyl)-2′,3′-*O*-isopropylidene-β-*D*-ribofuranosyl-9*H*-purine* (**8**). A soln. of **6** (1.275 g, 1.73 mmol) in dry CH_2Cl_2 (17 ml) was treated with Et_3SiH (2.21 ml, 13.84 mmol) and $ClCH_2COOH$ (1.71 ml, 20.76 mmol), and stirred for 1 h at 25°. The mixture was diluted with CH_2Cl_2 (10 ml) and H_2O (10 ml), and neutralised with 1M aq. NaOH. The aq. layer was extracted three times with AcOEt. The combined org. layers were dried (Na_2SO_4) and evaporated. FC (cyclohexane/AcOEt 1:1 → 1:2 → 1:4) gave **8** (550 mg, 68%). A sample for analysis was recrystallized from H_2O/MeCN. White solid. R_f (cyclohexane/AcOEt 1:2) 0.25. M.p. 95.1–95.4°. $[\alpha]_D^{25} = -1.9$ (*c* = 1.68, $CHCl_3$). UV ($CHCl_3$): 266 (14570). IR (ATR): 3197*w* (br.), 2985*w*, 2935*w*, 2876*w*, 1741*w*, 1606*m*, 1581*w*, 1520*w*, 1465*w*, 1434*w*, 1381*w*, 1373*m*, 1355*m*, 1327*w*, 1303*m*, 1252*m*, 1226*w*, 1206*w*, 1156*w*, 1125*w*, 1110*m*, 1075*s*, 1061*s*, 1054*s*, 1027*m*, 998*w*, 975*w*, 962*w*, 942*w*, 930*m*, 913*w*, 875*m*, 853*m*, 833*s*. ^{1}H-NMR (300 MHz, $CDCl_3$): see *Table 1*; additionally, 4.70 (br. *s*, $HOCH_2$–C(8)); 1.61, 1.38 (2*s*, Me_2C); 1.55 (*sept.*, *J* = 6.9, Me_2CH); 0.82 (*d*, *J* = 6.9, Me_2CH); 0.78 (*s*, Me_2CSi); 0.01 (*s*, Me_2Si). ^{13}C-NMR (75 MHz, $CDCl_3$): see *Table 7*; additionally, 114.88 (*s*, Me_2C); 34.11 (*d*, Me_2CH); 27.32, 25.49 (2*q*, Me_2C); 25.49 (*s*, Me_2CSi); 20.38, 20.35 (2*q*, Me_2CSi); 18.51 (*q*, Me_2CH); −3.41 (*q*, Me_2Si). HR-MALDI-MS: 465.2527 ($[M+H]^+$, $C_{22}H_{37}N_4O_5Si^+$; calc. 465.2533). Anal. calc. for $C_{22}H_{36}N_4O_5Si$ (464.63): C 56.87, H 7.81, N 12.06; found: C 57.15, H 7.76, N 12.04.

*8-(Chloromethyl)-5′-*O*-[dimethyl(1,1,2-trimethylpropyl)silyl]-2′,3′-*O*-isopropylidene-β-*D*-ribofuranosyl-9*H*-purine* (**9**). A soln. of **8** (541 mg, 1.16 mmol) in dry CH_2Cl_2 (8 ml) was cooled to 0°, treated with EtN(i-Pr)$_2$ (404 µl, 2.32 mmol) and MsCl (99 µl, 1.28 mmol), stirred at 25° for 18 h, treated with LiCl (49 mg, 1.16 mmol), and stirred for 8 h. The mixture was diluted with CH_2Cl_2 (8 ml), and washed three times with H_2O. The combined org. layers were dried (Na_2SO_4) and evaporated. FC (cyclohexane/AcOEt 9:1 → 4:1) gave **9** (537 mg, 96%). White solid. R_f (cyclohexane/AcOEt 1:1) 0.67. M.p. 81.0–82.0°. $[\alpha]_D^{25} = -23.1$ ($c = 1.4$, $CHCl_3$). UV ($CHCl_3$): 268 (10670). IR (ATR): 2993*w*, 2957*m*, 2875*w*, 1594*m*, 1581*m*, 1509*w*, 1466*w*, 1455*w*, 1425*w*, 1397*m*, 1373*m*, 1362*m*, 1307*w*, 1295*w*, 1251*m*, 1232*w*, 1212*m*, 1150*m*, 1122*m*, 1103*m*, 1073*s*, 1052*s*, 981*m*, 962*w*, 943*m*, 925*m*, 871*m*, 831*s*. ^{1}H-NMR (300 MHz, $CDCl_3$): see *Table 1*; additionally, 1.62, 1.40 (2*s*, *Me*$_2$C); 1.54 (*sept.*, $J = 6.9$, Me$_2$C*H*); 0.81 (*d*, $J = 6.9$, *Me*$_2$CH); 0.76, 0.75 (2*s*, Me$_2$CSi); −0.05 (*s*, Me$_2$Si). ^{13}C-NMR (75 MHz, $CDCl_3$): see *Table 7*; additionally, 114.56 (*s*, Me$_2$*C*); 34.16 (*d*, Me$_2$*C*H); 27.37, 25.55 (2*q*, *Me*$_2$C); 25.39 (*s*, Me$_2$CSi); 20.37, 20.34 (2*q*, *Me*$_2$CSi); 18.54, 18.52 (2*q*, *Me*$_2$CH); −3.42 (*q*, Me$_2$Si). HR-MALDI-MS: 483.2194 ($[M + H]^+$, $C_{22}H_{36}ClN_4O_4Si^+$; calc. 483.2189).

*5′-*O*-[Dimethyl(1,1,2-trimethylpropyl)silyl]-2′,3′-*O*-isopropylidene-β-*D*-ribofuranosyl-9*H*-purine-8-methyl-(8′ → 5′-*S*)-2′,3′-*O*-isopropylidene-5′-thiouridine* (**11**). A soln. of **9** (532 mg, 1.1 mmol) and **10** (377 mg, 1.1 mmol) in dry degassed MeOH (11 ml) was cooled to 0°, treated with a freshly prepared 0.66M soln. of MeONa in MeOH (5.0 ml, 3.3 mmol), and stirred at 25° for 3 h. The mixture was cooled to 0°, and treated with sat. aq. NH_4Cl soln. (20 ml). After evaporation of MeOH, the residue was extracted four times with AcOEt. The combined org. layers were dried (Na_2SO_4) and evaporated. FC (CH_2Cl_2/MeOH 95:5) gave **11** (802 mg, 98%). White solid. R_f (CH_2Cl_2/MeOH 95:5) 0.32. M.p. 95–97°. $[\alpha]_D^{25} = -58.2$ ($c = 0.78$, $CHCl_3$). UV ($CHCl_3$): 266 (18630). IR (ATR): 3192*w* (br.), 3054*w*, 2957*w*, 2937*w*, 2868*w*, 1691*s*, 1631*w*, 1597*w*, 1510*w*, 1455*m*, 1423*w*, 1375*m*, 1360*m*, 1303*w*, 1252*m*, 1211*m*, 1156*m*, 1076*s*, 971*m*, 923*w*, 860*m*, 828*s*. ^{1}H-NMR (300 MHz, $CDCl_3$): see *Table 2*; additionally, 7.30 (*d*, $J = 8.1$, H−C(6/I)); 5.71 (*dd*, $J = 8.1, 1.8$, H−C(5/I)); 1.61, 1.49, 1.40, 1.27 (4*s*, 2 Me$_2$C); 1.52 (*sept.*, $J = 6.9$, Me$_2$C*H*); 0.79 (*d*, $J = 6.9$, *Me*$_2$CH); 0.74, 0.73 (2*s*, Me$_2$CSi); −0.08 (*s*, Me$_2$Si). ^{13}C-NMR (75 MHz, $CDCl_3$): see *Table 8*; additionally, 114.79, 114.21 (2*s*, 2 Me$_2$*C*); 34.16 (*d*, Me$_2$*C*H); 27.33, 27.16, 25.53, 25.33 (4*q*, 2 *Me*$_2$C); 25.33 (*s*, Me$_2$CSi); 20.36, 20.35 (2*q*, *Me*$_2$CSi); 18.53 (*q*, *Me*$_2$CH); −3.43 (*q*, Me$_2$Si). HR-MALDI-MS: 747.3213 ($[M + H]^+$, $C_{34}H_{51}N_6O_9SSi^+$; calc. 747.3207).

Table 8. *Selected ^{13}C-NMR Chemical Shifts* [ppm] *of the ^{H}A*[s]U Dimers* **11** *and* **3** *in $CDCl_3$*

	11	**3**		**11**	**3**
Uridine unit (I)			Adenosine-derived unit (II)		
C(2/I)	154.53[a])	153.80[a])	C(2/II)	152.35	151.94
C(4/I)	163.46	163.36	C(4/II)	150.09[a])	150.03[a])
C(5/I)	102.87	102.90	C(5/II)	133.35	134.00
C(6/I)	142.62	142.53	C(6/II)	148.10	148.90
C(1′/I)	94.74	94.63	C(8/II)	152.16[a])	151.75[a])
C(2′/I)	84.46	84.40	CH_2−C(8/II)	28.49	28.64
C(3′/I)	83.34	83.17	C(1′/II)	90.09	92.22
C(4′/I)	87.02	86.65	C(2′/II)	82.83	82.74
C(5′/I)	33.63	33.85	C(3′/II)	81.89	81.62
			C(4′/II)	87.75	85.99
			C(5′/II)	62.85	63.30

[a]) Assignment may be interchanged.

*2′,3′-*O*-Isopropylidene-β-*D*-ribofuranosyl-9*H*-purine-8-methyl-(8′ → 5′-*S*)-2′,3′-*O*-isopropylidene-5′-thiouridine* (**3**). In a polyethylene flask, a soln. of **11** (696 mg, 0.93 mmol) in dry THF (4.7 ml) at 25° was treated with a soln. of $(HF)_3 \cdot Et_3N$ (1.53 ml, 28.0 mmol) and stirred at 25° for 64 h. The mixture was

cooled to 0°, treated with aq. 1M NaOH soln. until the pH reached *ca.* 10, and extracted four times with AcOEt. The combined org. layers were dried (Na_2SO_4) and evaporated. FC (CH_2Cl_2/MeOH 97:3) gave **3** (533 mg, 95%). White solid. R_f (CH_2Cl_2/MeOH 97:3) 0.40. M.p. 126.0–129.5°. $[\alpha]_D^{25} = -47.2$ ($c = 0.73$, $CHCl_3$). UV ($CHCl_3$): 265 (16760). IR (ATR): 3496*w* (sh.), 3219*w* (br.), 3058*w*, 2987*w*, 2937*w*, 2876*w*, 2823*w*, 1688*s*, 1631*w*, 1598*m*, 1510*w*, 1456*m*, 1425*w*, 1374*m*, 1362*m*, 1303*w*, 1266*m*, 1212*m*, 1155*m*, 1077*s*, 987*m*, 946*w*, 854*m*, 810*m*. ^{1}H-NMR (300 MHz, $CDCl_3$): see *Table 2*; additionally, 7.26 (*d*, $J = 8.1$, H–C(6/I)); 5.68 (*dd*, $J = 8.1$, 1.7, H–C(5/I)); 5.61 (*dd*, $J = 11.0$, 2.0, HO–C(5′/II)); 1.64, 1.47, 1.37, 1.24 (4*s*, 2 Me_2C). ^{13}C-NMR (75 MHz, $CDCl_3$): see *Table 8*; additionally, 114.83, 114.45 (2*s*, 2 Me_2*C*); 27.83, 27.12, 25.47, 25.26 (4*q*, 2 *Me*$_2$C). HR-MALDI-MS: 627.1853 ($[M + Na]^+$, $C_{26}H_{32}N_6NaO_9S^+$; calc. 627.1849).

Evaluation of the Solubility and Gelation Properties. In a 5-ml vial closed with a stopper, a mixture of 5 mg of the dimers **1**, **2**, or **3**, and 500 µl of the solvent was stirred at 75° (95° when decanol was used). A compound was considered *insoluble*, when no complete dissolution occurred upon heating for *ca.* 10 min. A compound was considered as *soluble*, when a soln. was obtained upon heating, and remained a soln. after 36 h at 25°. A mixture of a compound and a solvent was considered a *gel* when, after dissolution upon heating, followed by cooling to 25°, no flowing could be observed upon inversion of the vial ('stable to inversion' criterion) [48]. A *partial gel* refers to a jelly-like soln. that shows a significant flow upon inversion of the vial.

Determination of the Gel–Sol Transition Temperature (T_m). A vial containing a gel was placed in a thermostated bath, and the temp. was slowly increased by steps of 1°. T_m was considered to be reached when the material flowed upon inversion of the vial.

Determination of the Minimum Gelation Concentration (MGC). MGC was determined by addition of a defined amount of solvent to a vial containing a gel, so as to reduce the gelator concentration in steps of 0.1% (*w*/*v*). The mixture was then heated above T_m, until a clear soln. was obtained, and the sample was cooled to 25°. The process was repeated until the material flowed upon inversion of the vial.

Rheological Characterisation of the Gels. All measurements were performed on a *Anton Paar Physica MCR 300* rheometer equipped with a cone-plate system *CP 30-4* (49.95-mm diameter, 4.0° angle). The storage and loss moduli were not corrected, due to the inaccurate measurement of the effective radius of the sample. The amplitude sweeps were performed at increasing and decreasing strains (1 min pause between the experiments), at constant temp. (25°) and frequency (1 Hz). The limiting value of the linear viscoelastic range, γ_L, was determined manually with a tolerated deviation of 5%. The temp. sweeps were performed in a chamber containing an atmosphere saturated with solvent vapours, at increasing temp. (rate 5–10°/min), and constant strain (0.3%) and frequency (1 Hz).

CD Spectra of the Gels. The gel was heated above its T_m, rapidly transferred as a soln. to a 1-mm path-length cell, and kept at 25° until gelation occurred (10 min to 3 h). The CD measurements were performed on a *Jasco J-710* spectropolarimeter, at increasing temp., using the following settings: 10-nm bandwidth, 0.5-s response, low sensivity, 0.1-nm data pitch, and 50–200-nm/min scanning speed.

REFERENCES

[1] S. Eppacher, N. Solladié, B. Bernet, A. Vasella, *Helv. Chim. Acta* **2000**, *83*, 1311.
[2] X. Zhang, B. Bernet, A. Vasella, *Helv. Chim. Acta* **2006**, *89*, 2861.
[3] X. Zhang, B. Bernet, A. Vasella, *Helv. Chim. Acta* **2007**, *90*, 864.
[4] X. Zhang, B. Bernet, A. Vasella, *Helv. Chim. Acta* **2007**, *90*, 891.
[5] A. J. Matthews, P. K. Bhardwaj, A. Vasella, *Helv. Chim. Acta* **2004**, *87*, 2273.
[6] A. Ritter, D. Egli, B. Bernet, A. Vasella, *Helv. Chim. Acta* **2008**, *91*, 673.
[7] A. Viger, Ph.D. Thesis No. 16060, ETH-Zürich, 2005.
[8] K. Araki, I. Yoshikawa, *Top. Curr. Chem.* **2005**, *256*, 133.
[9] N. M. Sangeetha, U. Maitra, *Chem. Soc. Rev.* **2005**, *34*, 821.
[10] J. H. van Esch, B. L. Feringa, in 'Encyclopedia of Supramolecular Chemistry', Eds. J. L. Atwood, J. W. Steed, Marcel Dekker, New York, Basel, 2004, p. 586–596.
[11] P. J. Flory, *Faraday Discuss. Chem. Soc.* **1974**, *57*, 7.
[12] O. Gronwald, E. Snip, S. Shinkai, *Curr. Opin. Colloid Interface Sci.* **2002**, *7*, 148.

[13] D. J. Abdallah, R. G. Weiss, *Adv. Mater.* **2000**, *12*, 1237.
[14] P. Terech, R. G. Weiss, *Chem. Rev.* **1997**, *97*, 3133.
[15] M. de Loos, B. L. Feringa, J. H. van Esch, *Eur. J. Org. Chem.* **2005**, 3615.
[16] L. A. Estroff, A. D. Hamilton, *Chem. Rev.* **2004**, *104*, 1201.
[17] K. Y. Lee, D. J. Mooney, *Chem. Rev.* **2001**, *101*, 1869.
[18] T. Kato, Y. Hirai, S. Nakaso, M. Moriyama, *Chem. Soc. Rev.* **2007**, *36*, 1857.
[19] T. Kato, N. Mizoshita, M. Moriyama, T. Kitamura, *Top. Curr. Chem.* **2005**, *256*, 219.
[20] M. George, R. G. Weiss, *Acc. Chem. Res.* **2006**, *39*, 489.
[21] A. Ajayaghosh, V. K. Praveen, *Acc. Chem. Res.* **2007**, *40*, 644.
[22] V. Nair, S. D. Chamberlain, *Synthesis* **1984**, 401.
[23] A. Ritter, B. Bernet, A. Vasella, *Helv. Chim. Acta* **2008**, *91*, 1675.
[24] H. Gunji, A. Vasella, *Helv. Chim. Acta* **2000**, *83*, 1331.
[25] H. S. Gutowsky, A. Saika, *J. Chem. Phys.* **1953**, *21*, 1688.
[26] A. Dunger, H. H. Limbach, K. Weisz, *Chem. – Eur. J.* **1998**, *4*, 621.
[27] H. Iwahashi, Y. Kyoguku, *J. Am. Chem. Soc.* **1977**, *99*, 7761.
[28] Y. Kyogoku, R. C. Lord, A. Rich, *J. Am. Chem. Soc.* **1967**, *89*, 496.
[29] M. Chastrette, M. Rajzmann, M. Chanon, K. F. Purcell, *J. Am. Chem. Soc.* **1985**, *107*, 1.
[30] T. Sato, M. Seko, R. Takasawa, I. Yoshikawa, K. Araki, *J. Mater. Chem.* **2001**, *11*, 3018.
[31] E. Snip, K. Koumoto, S. Shinkai, *Tetrahedron* **2002**, *58*, 8863.
[32] Y. J. Yun, S. M. Park, B. H. Kim, *Chem. Commun.* **2003**, 254.
[33] I. Yoshikawa, S. Yanagi, Y. Yamaji, K. Araki, *Tetrahedron* **2007**, *63*, 7474.
[34] Y. Jeong, K. Hanabusa, H. Masunaga, I. Akiba, K. Miyoshi, S. Sakurai, K. Sakurai, *Langmuir* **2005**, *21*, 586.
[35] G. John, G. Zhu, J. Li, J. S. Dordick, *Angew. Chem., Int. Ed.* **2006**, *45*, 4772.
[36] R. Luboradzki, O. Gronwald, A. Ikeda, S. Shinkai, *Chem. Lett.* **2000**, 1148.
[37] G. Y. Zhu, J. S. Dordick, *Chem. Mater.* **2006**, *18*, 5988.
[38] C. Reichardt, in 'Solvents and Solvent Effects in Organic Chemistry', Wiley-VCH, Weinheim, 2003, p. 389 – 469.
[39] C. Reichardt, *Chem. Rev.* **1994**, *94*, 2319.
[40] R. Brummer, in 'Rheology Essentials of Cosmetic and Food Emulsions', Springer-Verlag, Berlin, 2006, p. 63 – 80.
[41] T. Mezger, in 'The rheology handbook: for users of rotational and oscillatory rheometers', Ed. U. Zorll, Vincentz Verlag, Hannover, 2002, p. 122 – 126.
[42] G. Gottarelli, G. Spada, E. Castiglioni, in 'Molecular Gels: Materials with Self-Assembled Fibrillar Networks', Eds. R. G. Weiss, P. Terech, Springer-Verlag, Dordrecht, 2006, p. 431 – 446.
[43] P. R. Callis, *Annu. Rev. Phys. Chem.* **1983**, *34*, 329.
[44] P. S. Song, *Ann. Rep. Prog. Chem., Sect. B: Org. Chem.* **1977**, *74*, 18.
[45] C. A. Bush, H. A. Scheraga, *Biopolymers* **1969**, *7*, 395.
[46] C. S. M. Olsthoorn, C. A. G. Haasnoot, C. Altona, *Eur. J. Biochem.* **1980**, *106*, 85.
[47] M. Simonyi, Z. Bikádi, F. Zsila, J. Deli, *Chirality* **2003**, *15*, 680.
[48] S. R. Raghavan, B. H. Cipriano, in 'Molecular Gels: Materials with Self-Assembled Fibrillar Networks', Eds. R. G. Weiss, P. Terech, Springer-Verlag, Dordrecht, 2006, p. 241 – 252.

Received July 10, 2008